

2017

# Origin of Graphite in the Southwestern Grenville Province

Mehmet F. Taner

Cameron Drever  
*University of Waterloo*

Chris Yakymhuk  
*University of Waterloo*

Fred Longstaffe  
*The University of Western Ontario, flongsta@uwo.ca*

Follow this and additional works at: <https://ir.lib.uwo.ca/earthpub>

 Part of the [Geochemistry Commons](#), and the [Geology Commons](#)

---

## Citation of this paper:

Taner, Mehmet F.; Drever, Cameron; Yakymhuk, Chris; and Longstaffe, Fred, "Origin of Graphite in the Southwestern Grenville Province" (2017). *Earth Sciences Publications*. 24.  
<https://ir.lib.uwo.ca/earthpub/24>

# ORIGIN OF GRAPHITE IN THE SOUTHWESTERN GRENVILLE PROVINCE

MEHMET F. TANER

*1107 Gablefield Private, Gloucester, Ontario K1J 1E4*

CAMERON DREVER & CHRIS YAKYMCHUK\*

*Department of Earth and Environmental Sciences, University of Waterloo, 200 University Ave  
West, Waterloo, Ontario, N2L 3G1*

*\*cyakymchuk@uwaterloo.ca*

FRED J. LONGSTAFFE

*Department of Earth Sciences, The University of Western Ontario, London, Ontario N6A5B7,  
Canada*

## ABSTRACT

Two graphite deposits in the southwestern Grenville Province are investigated to evaluate the origin of graphitic carbon and test if graphite mineralization is syngenetic or epigenetic. Graphite mineralization in the Bissett Creek deposit is characterized by homogeneously distributed and disseminated graphite flakes (about 1 to 5 mm in size and 2 to 10 vol.%) within graphitic gneisses. Graphite flakes are intergrown with metamorphic minerals, most notably biotite. The Montpellier Graphite showing in Quebec contains graphite concentrations of up to 20 vol.%. In contrast to the disseminated and homogeneously distributed graphite in the Bissett Creek Deposit, graphite mineralization at Montpellier forms lenses of variable sizes that occur at the top of a calc-silicate unit and as graphite-rich lenses in biotite-sillimanite rich paragneiss. The  $\delta^{13}\text{C}$  of graphite ranges from  $-29$  to  $-17$  ‰ at Bissett Creek and from  $-18$  to  $-14$  ‰ at Montpellier. Carbon isotope compositions of graphite from both deposits support a biogenic source for the carbon and the spread in  $\delta^{13}\text{C}$  can be generated through Rayleigh fractionation. A minor

contribution of inorganic carbon from the devolatilization of carbonate minerals is possible at Montpellier. Mineralization at Bissett Creek and Montpellier is interpreted to represent syngenetic graphite mineralization from organic-rich material during high-temperature metamorphism.

*Keywords:* Graphite, Grenville Province, Carbon isotopes, Metamorphic, Gneiss

## INTRODUCTION

As an industrial mineral, graphite is primarily utilized in the steel industry where it is included in bricks that line furnaces (*e.g.*, refractories) to provide strength and resistance to heat and corrosion, used to line ladles and crucibles, and added to steel to increase strength (Luque *et al.* 2014). Graphite is also used extensively in the automobile industry in gaskets, brake linings and clutch materials. It has a myriad of other industrial uses including electric motors (carbon brushes), batteries, lubricants, pencils, fuel cells, vanadium redox batteries, components of equipment used to generate nuclear and solar energy, golf clubs, hockey sticks, and other sporting goods (*cf.*, Spence 1920, Hewitt 1965, Garland 1987, Mackinnon & LeBaron 1992). Increasing demand for green energy has also made graphite a very attractive exploration prospect because of its abundant use in lithium-ion batteries. Thus, it is important to develop and test genetic models of graphite mineralization, which can be used to prioritize exploration targets.

Graphite deposits are usually divided into three classes. From relatively low to high value, these classes include: amorphous, flake and vein graphite deposits (Spence 1920, Mitchell 1993, Luque *et al.* 2014). Amorphous graphite represents an aggregate of extremely fine lathes. Flake graphite is the scaly or lamellar form of the mineral, commonly found disseminated in

metamorphic rocks, such as crystalline limestone, gneisses and schist (*e.g.* Mitchell 1993). Vein graphite is found in veins or fracture systems along intrusive contacts of pegmatites with host limestones and schists (*e.g.* Luque *et al.* 2014).

There are currently two main genetic models that describe graphite mineralization. They are the growth of graphite during metamorphic processes, also known as graphitization, and the precipitation of graphite from hydrothermal fluids or melt (Rumble *et al.* 1986a,b, Papineau *et al.* 2010a, b, Luque *et al.* 2012, Beyssac & Rumble 2014,). These processes are end members; some graphite deposits are formed through both metamorphism and hydrothermal deposition (Papineau *et al.* 2010a,b, Luque *et al.* 2012). Graphitic carbon deposited from hydrothermal fluids occurs globally, in rocks from all depths in Earth's crust and ranging in age from Precambrian to Tertiary (Rumble 2014). Metamorphic graphite is concentrated in high-temperature metamorphic rocks whereas lower-grade rocks generally contain other carbonaceous material (*e.g.* coal) in addition to graphite (Okuyama-Kusunose and Itaya, 1987)

In the Southwestern Grenville Province, it is unclear if Proterozoic graphite deposits are formed through metamorphic or hydrothermal processes or some combination of both. This is important information for understanding the genesis of graphite (*e.g.*, Luque *et al.* 2014) and linking metamorphism into global geochemical cycles of carbon (*e.g.*, Galy *et al.* 2008). Also, understanding the mineralization mechanisms and the influence of different rock types and structures can be used to develop new exploration targets for graphite deposits (*e.g.*, Soman *et al.* 1986). In this contribution, the origin of two graphite deposits in the southwestern Grenville Province (the Bissett Creek deposit in Ontario and the Montpelier graphite showing in Quebec) are evaluated using a combination of field observations, petrology, litho-geochemistry and carbon isotope analysis of graphite. These locations were chosen because the rocks at the Bissett Creek

deposit contain no carbonate minerals whereas graphite mineralization at the Montpellier showing is spatially associated with carbonates. Two possible sources for carbon that form graphite in metamorphic terranes are the breakdown of organic material to graphite at temperatures at and above the amphibolite facies (e.g. Landis, 1971), and the decarbonation of carbonate minerals and precipitation of graphite at amphibolite- to granulite-facies conditions (e.g. Santosh and Omori, 2008). Therefore, this investigation of the Bissett creek deposit and the Montpellier showing allows the two main models of graphite mineralization to be evaluated for two different styles of graphite deposits in the southwestern Grenville Province.

## REGIONAL GEOLOGY

Most graphite mineralization in Canada is located in the Grenville Province of Southern Quebec and Central Ontario (Spence 1920, Hewitt 1965, Garland 1987, Simandl 1989, Mackinnon & LeBaron 1992). The metallogeny of the structural zones of the Grenville province was well defined by Sangster *et al.* (1992). The southwestern Grenville Province consists of granitic gneisses, metavolcanic rocks, metasedimentary schists and impure marbles that were deformed and metamorphosed during the Grenville orogen (Wynne-Edwards 1972, Carr *et al.* 2000, Rivers *et al.* 2012).

The two graphite deposits studied here are located in separate parts of the southwestern Grenville Province. The Bissett Creek deposit is part of the Mesoproterozoic gneisses of the Central Gneiss Belt (Carr *et al.* 2000), which is also known as the Ottawa River Gneiss Complex (Rivers & Schwerdtner 2015). In the vicinity of the deposit, the geology is interpreted to represent reworked rocks of the former Laurentian margin (e.g., Carr *et al.* 2000). The Montpellier graphite showing is found in the Composite Arc Belt, which represents

allochthonous Mesoproterozoic volcanic arcs and sedimentary rocks that accreted to the southeast margin of Laurentia during the Grenville orogen (*e.g.*, Carr *et al.* 2000).

## GEOLOGY OF THE BISSETT CREEK GRAPHITE DEPOSIT

### *Location*

The Bissett Creek graphite property (Fig. 1) belongs to the Northern Graphite Corporation of Ottawa and it is easily accessible by the Trans-Canada Highway (Highway 17), approximately 53 km east of the town of Mattawa. All mining claims are located in Maria Township, Ontario in the County of Renfrew, Province of Ontario.

### *Field relationships and lithogeochemistry*

Graphite mineralization at the Bissett Creek deposit is characterized by homogeneously distributed graphite flakes (about 1 to 5 mm in size) within biotite-rich quartzofeldspathic gneisses (Fig. 2a; Taner 2010, 2013). The graphitic gneisses are subdivided into: (1) biotite-rich quartzofeldspathic gneiss, (2) diopside–tremolite–biotite graphitic gneiss, and (3) graphite-poor sillimanite–garnet gneiss, which occurs at the boundary between the graphitic and barren gneisses. Where observed, the contacts between each of the different graphitic gneiss units are gradational over centimetres to metres. The total thickness of graphitic gneisses, from west to east, varies from 25 m to 90 m, as determined by drilling. At the surface, the graphitic gneisses form a distinctive recessive weathering unit (generally red-orange to pale yellow-brown weathering) and are commonly exposed along rock cuts, hilltops and occasional cliff faces (Fig. 2b). When weathered, graphite flakes are easily picked out of the rock.

A barren quartzofeldspathic gneiss with no graphite occurs structurally above and below the graphitic gneiss. Drilling intersections internal to the deposit vary in thickness from 1 to 20 m. In drill core, sharp contacts between the barren gneiss and the graphitic gneiss suggest an intrusive relationship. The gneissic units are intruded by metre-scale pegmatites (Fig. 2c), and in one location, by a metre-scale lamprophyre dyke (Fig. 2d).

The pegmatite unit is a light grey to pinkish, quartz-feldspar rich rock with some large dark brown flakes of biotite and rare pyrite. Pegmatite zones locally contain rare graphite mineralization in the form of flakes intercalated with biotite. Biotite enrichment occurs within the contact zones with the host gneisses.

The lamprophyre dyke unit is fine grained, dark green and exhibits sharp intrusive contacts with the graphitic and barren gneiss units. The lamprophyre dykes do not contain graphite mineralization. Lamprophyre dykes are subvertical and generally strike east–west (Fig. 2d).

Foliations are shallowly dipping to sub-horizontal across the property. The graphitic gneiss has a moderate dip to the east from 5 to 20 degrees and the high-grade layer dips 20 to 30 degrees south. Gignac et al. (2012) report two generations of folding present on the property. The primary deformation event produced isoclinal folds (Fig. 2a), which were then refolded during a second event into large open folds (Gignac *et al.* 2012).

#### *Petrographic observations*

The biotite-rich, quartzofeldspathic graphitic gneiss is fine to medium-grained, light to dark grey, and contains between 2 and 10 vol.% homogeneously disseminated, graphite flakes (Fig. 3a). The biotite-rich, quartzofeldspathic gneiss is composed of centimetre-to decimetre-

scale, quartz-feldspar rich leucosomes that have lower amounts of graphite and display augen-  
gneiss textures. Leucosomes alternate with millimetre- to centimetre-scale biotite and graphite-  
rich layers. Biotite-rich layers contain between 4 and 10 vol.% graphite that is homogeneously  
distributed (Fig. 4a). Graphite flakes are 1–5 mm in length (Fig. 4b) and are intimately associated  
with biotite (Fig. 4c). Disseminated sulfides (1–2 vol.%, mostly pyrrhotite) occur within biotite-  
rich layers. Garnet and muscovite are present in some samples from this unit.

The diopside–tremolite–biotite gneiss is fine- to medium-grained and is composed of  
quartz–feldspar-rich layers (mm to dm) that alternate with diopside–tremolite–biotite–graphite  
rich layers (Fig. 3b). It is located in the upper part of the mineralized graphite zones at Bissett  
Creek. Graphite comprises 3 to 6 vol.% of this unit and is homogeneously distributed as  
disseminated graphite flakes (Fig. 4d). Trace amounts (1–2 vol.%) of disseminated sulfide  
minerals (mostly pyrrhotite) are also present. Some parts of this unit also contain garnet, but it is  
frequently found in close association with pegmatite intrusions. Minerals are generally  
granoblastic in this unit.

The biotite–sillimanite–garnet gneiss unit is medium-grained and contains a well-defined  
foliation defined by the parallel alignment of biotite and sillimanite lathes (Fig. 3c). It is  
composed of millimetre- to centimetre-scale, leucocratic layers that alternate with millimetre- to  
decimetre-scale, biotite–sillimanite–garnet-rich layers. The melanocratic layers are composed of  
quartz and feldspar with up to 15 vol.% biotite, up to 15 vol.% sillimanite and up to 5 vol.%  
garnet. Graphite flakes are rare and are usually associated with disseminated pyrite and  
pyrrhotite (1–2 vol.%).



The barren gneiss unit is found structurally above and below the graphitic gneiss units. This unit is composed of pink quartzofeldspathic leucosome that alternates with relatively biotite-rich melanosome (Fig. 3d). This unit contains no graphite.

#### *Economic Geology*

The graphitic carbon contents of select graphitic units reported in Gignac *et al.* (2012) are summarized in Table 1 and displayed in Figure 5. Samples were analyzed for graphitic carbon at SGS Laboratories using the CSA05V analytical package, which uses a roast/coulometry method. The diopside–tremolite–biotite gneiss shows a range of graphitic carbon contents from ~1 to 3 wt.%. The biotite-rich quartzofeldspathic gneiss unit contains between ~1 and 4 wt.% graphitic carbon. The median graphitic carbon content of the biotite-rich quartzofeldspathic gneiss is ~1% higher than the diopside–tremolite–biotite gneiss (Fig. 5). Graphite particles generally contain 20–30 vol.% interlayered mica (Fig. 4c). Measured resources of graphite at the Bissett Creek deposit are estimated at 69.8 million tonnes grading 1.74% graphitic carbon based on a 1.02% graphitic carbon cutoff grade (Gignac *et al.* 2012, Leduc 2013). The inferred resource is 24 million tonnes grading 1.65% graphitic carbon with a 1.02% graphitic carbon cutoff (Gignac *et al.* 2012, Leduc 2013). Liberated graphite flakes occur as oval to sub-rounded particles ranging from 1 to 6 mm in diameter.

#### GEOLOGY OF THE MONTPELLIER GRAPHITE OCCURRENCE

##### *Location*

The Montpellier Graphite showing is located northeast of Lavergne Lake close to the village of Montpellier in Ripon Township, within the Composite Arc Belt of the Grenville Province (Fig. 1).

#### *Field Relationships*

The geology of the Montpellier graphite showing is summarized in a simplified stratigraphic column in Figure 6. The geology consists of metasedimentary rocks (quartzite, paragneiss, and calc-silicate), metavolcanic rocks (both mafic and felsic), and granitic gneisses and an ortho-amphibolite. These units have experienced polyphase folding (Fig. 7a, b). All units are crosscut by a diabase dyke.

The graphite-rich unit contains up to 20 vol.% graphite and forms lenses of variable sizes at the top of a calc-silicate unit and also within biotite–sillimanite–garnet-rich paragneiss (Fig. 6). Disseminated graphite also occurs in the calc-silicate unit (Fig. 7a). The contact between the graphite-bearing paragneiss unit and the overlying impure quartzite unit is irregular (Fig. 7c).

The graphite showing is exposed at surface along a vertical cliff about 4 m high and over a distance of 100 m. This zone is strongly oxidized (Fig. 7b), contains sulfide minerals (mostly pyrrhotite and lesser amounts of pyrite), and it is very friable and weathered along this exposure. Graphite is visible as dark flakes within the competent gneissic unit and when it is weathered, similar to Bissett Creek, graphite flakes are easily picked out of the rock. Graphite flakes are preferentially aligned with the gneissosity. In this particular part of the showing the gneissosity dips shallowly to the west (Taner 1989).

#### *Petrographic observations*

The graphite-rich unit contains up to 15–25 vol.% graphite. Two types of mineralization are distinguished: (1) a massive zone with uniformly distributed graphite flakes; and (2) a zone where the graphite flakes are concentrated in nodules. The massive zone occurs in both calc-silicate and paragneiss units whereas the nodular zone is only found in the paragneiss unit.

The calc-silicate unit contains 3–5 vol.% disseminated graphite (Fig. 7a). This unit is composed of variable quantities of recrystallized carbonate (calcite and/or dolomite, about 30–50 vol.%; Fig. 8a), diopside (20–30 vol.%), plagioclase (20–30 vol.%) and minor amounts of wollastonite, scapolite, phlogopite, sulfides (pyrrhotite and/or pyrite), and disseminated graphite flakes (3–5 vol.%). Locally, the amount of disseminated graphite can reach 20 vol.% (Fig. 8b). Disseminated grains (or blebs) of sphalerite (mm to cm in size) occur within the calc-silicate unit. Graphite mineralization is stratiform at the top of calc-silicate unit.

Biotite–sillimanite–garnet-rich paragneiss lies beneath the most graphite-rich horizon (Fig. 6). From the contact with the lower calc-silicate unit, the proportion of graphite flakes progressively increases up section within biotite-rich paragneiss. This unit contains coarse-grained garnet and biotite. Graphite is intergrown with biotite (Fig. 8c, d) and is found along cracks in garnet (Fig. 8c).

### *Economic Geology*

The graphitic carbon contents of the graphitic units from the main outcrop are summarized in Table 2. Samples were analyzed for graphitic carbon at SGS Laboratories using the CSA05V analytical package. Graphitic carbon contents range from ~1 to 20 wt.%, with more than half the values above 10 wt.%. Individual graphite grains are millimeters in length (Fig. 8e, f). The average grade of this main outcrop is 13.6 wt.% graphitic carbon. Graphite mineralization

continues beneath the impure quartzite unit and within the biotite–sillimanite–garnet-rich paragneiss. Mineralized zones vary in thickness from 0.2 to 4.8 m and are laterally continuous over 100 m. Graphite-rich zones are composed of friable material that form lenses with graphite flakes of about 1 mm in size.

## CARBON ISOTOPE ANALYSIS OF GRAPHITE

### *Methods*

Twelve samples were selected for carbon isotope analysis of graphite (eight from Bissett Creek and four from Montpellier). Six samples from Bissett Creek were sampled from drill core, one from a hand sample (BC-0) and one was a graphite concentrate from the mill (BC-M). Four samples were collected from drill core from the Montpellier prospect. With the exception of the mill sample from Bissett Creek, all rocks were crushed by hand and graphite was hand-picked under a binocular microscope. For the mill sample, an aliquot of the graphite product was used.

The carbon isotopic compositions of the graphite separates were analyzed at the Laboratory for Stable Isotope Science at the University of Western Ontario. The refractory nature of the graphite presented challenges for some samples and hence a range of analytical approaches were used. First, all samples were analyzed using a Costech 4010 Elemental Analyzer connected in continuous flow mode to a Thermo Scientific Delta<sup>PLUS</sup> XL mass spectrometer. About 0.2 – 0.6 mg of sample was wrapped in tin capsules, prior to combustion at 1020°C. These analyses were conducted twice, once without and once with addition of ~1 mg of V<sub>2</sub>O<sub>5</sub>. The latter was added as extra oxidant to facilitate combustion. Samples were calibrated to VPDB using the accepted values for USGS40 and USGS41 (Qi *et al.* 2003).

Ten of twelve samples were also analyzed using the conventional method of Boutton (1991). Graphite (~1.2 – 1.5 mg) was added to a quartz tube, along with 600 mg of CuO and 500 mg Cu. The evacuated and sealed quartz tubes were then combusted at 900°C for two hours and cooled overnight. Because visible graphite still remained in the quartz tubes, they were combusted again for a further 3 hours at 1000°C, prior to being allowed to cool overnight. The carbon dioxide was then released, cryogenically purified, and then analyzed using a Micromass Optima dual inlet isotope ratio mass spectrometer. Samples were calibrated to VPDB using accepted values for NBS-19 and L-SVEC (Coplen *et al.* 2006a).

All results are reported in the normal delta notation relative to VPDB (Coplen *et al.*, 2006b). Comparable results were obtained for all methods. A  $\delta^{13}\text{C}$  of  $-15.9 \pm 0.2\text{‰}$  (2SD; n=8) was obtained for USGS24 graphite, as compared to its accepted value  $-16.0 \pm 0.1\text{‰}$  (2SD). A  $\delta^{13}\text{C}$  of  $-25.7 \pm 0.2\text{‰}$  (SD; n=5) was obtained for the internal laboratory carbon standard, as compared to its accepted value of  $-25.7 \pm 0.2\text{‰}$  (SD). Reproducibility (SD) of samples ranged from  $\pm 0.1$  to  $\pm 0.7 \text{‰}$ , and averaged  $\pm 0.3\text{‰}$  (Table 3).

## Results

The  $\delta^{13}\text{C}$  of graphite in this study is summarized in Table 3 and in Figure 9. For the Bissett Creek deposit, the carbon isotope compositions have a wide range, varying from  $-29$  to  $-17\text{‰}$  and yield an average value of  $-23\text{‰}$ . For the Montpellier showing, measured compositions range from  $-18$  to  $-14\text{‰}$  with an average of  $-16\text{‰}$ .

## DISCUSSION

### *Metamorphic versus hydrothermal graphite*

Graphite deposits may form through metamorphism of carbonaceous matter or by precipitation from carbonic fluids and/or melts (Pasteris 1999, Luque *et al.* 2014). Syngenetic (or ‘metamorphic’) graphite deposits are generally found in high-grade metamorphic rocks and the graphite is disseminated in flake form (Luque *et al.* 2014). Individual graphite grains usually contain impurities of metamorphic minerals (Mitchell 1993) and graphite is found within the matrix assemblage and not in pore spaces (Bernard & Papineau 2014). The carbon content of graphite in these deposits generally ranges from 75 to 97% and individual crystals are generally millimeters in size (Mitchell 1993).

Epigenetic (or ‘vein graphite’) deposits are also usually found in high-grade metamorphic rocks, but they are spatially associated with fracture or vein sets (*e.g.* Rumble and Hoering 1986b, Kehelpannala & Francis 2001). Graphite in these deposits is nearly pure with average carbon contents of ~99% (Mitchell 1993). Graphite occurs as nearly monomineralic veins or nodules that are centimeters to decimeters in size (Barrenechea *et al.* 2009, Luque *et al.* 2014). Individual crystals are large and generally centimeters in size (Mitchell 1993).

Four specific petrographic and field observations support the metamorphic (syngenetic) model for graphite mineralization at both Bissett Creek and Montpellier. First, graphite is disseminated throughout the graphitic units and is not located along fracture sets or associated with veins. At Montpellier, some graphite occurs in nodules, but graphite represents less than 30 vol.% of the mineral assemblage, which is inconsistent with nearly monomineralic veins that are characteristic of epigenetic graphite deposits. Second, individual graphite flakes from Bissett Creek and Montpellier can contain up 20–30 vol.% interlayered biotite. Again, this is incompatible with the relatively pure (~99%) graphite from epigenetic deposits. Third, individual graphite flake sizes are on the order of millimeters, which is consistent with other syngenetic

graphite deposits (*e.g.* Mitchell 1993). Fourth, graphite flakes are intergrown with metamorphic minerals including biotite and garnet (Fig. 4c, 8c), which supports a metamorphic origin for the graphite. Taken together, these different petrological and field observations are most consistent with a metamorphic model of graphite mineralization and are incompatible with the epigenetic model of graphite deposition.

#### *Origin of carbon responsible for graphite mineralization*

There are three main sources of carbon that form graphite: (1) carbon from organic materials, (2) carbon from the devolatilization of carbonate minerals, and (3) carbon from mantle sources (Luque *et al.* 2012). Each of these sources has a characteristic range of  $\delta^{13}\text{C}$ . Most Proterozoic organic matter has  $\delta^{13}\text{C}$  that ranges from  $-40$  to  $-10$  ‰ (Schidlowski 1988, 2001). The  $\delta^{13}\text{C}$  of carbon derived from the mantle is approximately  $-5$  ‰ (*e.g.*, Deines 2002). Marine carbonates generally have compositions around  $\sim 0$  ‰ (*e.g.*, Keith & Weber 1964). The compositions of these sources are summarized in Figure 9. The carbon isotope compositions of these sources, however, can only be compared with measured graphite  $\delta^{13}\text{C}$  if the latter has not been significantly fractionated during metamorphism.

There are two main processes that can modify the carbon isotope composition of graphite from that of its source during metamorphism. Devolatilization of organic material can shift  $\delta^{13}\text{C}$  by up to 5‰ (*e.g.*, Barker & Friedman 1969, Wada *et al.* 1994), usually due to the release of isotopically light carbon during the production of methane (*e.g.*, Luque *et al.* 2012). Most studies, however, document shifts of  $\sim 1$ ‰ (*e.g.*, Hahn-Weinheimer & Hirner, 1981). The second process is carbon isotope exchange between graphite and inorganic material (*e.g.* carbonate minerals).

The presence of two carbonic species during metamorphism (organic carbon and carbonate minerals and/or carbonic fluid derived from their breakdown) with different carbon isotope compositions leads to isotopic exchange during metamorphism. The amount of isotope fractionation during carbon isotope exchange is mainly a function of temperature (Dunn & Valley 1992). This process is particularly important at relatively low metamorphic temperatures. For example, the calibration of Dunn & Valley (1992) for calcite–graphite isotope exchange predicts shifts of ~10‰ at 400°C and ~6‰ at 600°C. High-temperature metamorphism (e.g. amphibolite and granulite facies) promotes efficient isotope exchange between these minerals and isotope fractionation is expected to be only a few per mil (e.g., Dunn & Valley 1992). This is supported by graphite in metamorphic rocks that has  $\delta^{13}\text{C}$  similar to the primary organic material inferred to be the source of carbon (e.g., Barker & Friedman 1969, Weis *et al.* 1981, Crawford & Valley 1990). Because mineralization at Bissett Creek and Montpellier occurs in amphibolite-to granulite-facies gneisses (see Rivers *et al.* 2012 and references therein), the carbon isotope compositions of graphite from Bissett Creek and Montpellier are expected to be within a few per mil of that of the source of the carbon.

The  $\delta^{13}\text{C}$  compositions of graphite from both deposits show a continuum of values from –29 to –14‰ that is consistent with carbon derived from organic materials (Schidlowski 1988, 2001). Graphite from Montpellier is enriched in  $^{13}\text{C}$  relative to graphite from Bissett Creek, which may reflect a more  $^{13}\text{C}$ -rich source of carbon or isotopic exchange between carbonate minerals and graphite. Although carbonate minerals are not currently present at the Bissett Creek deposit, the diopside–tremolite–biotite assemblage in the calc-silicate unit was likely derived from decarbonation reactions involving the breakdown of calcite and dolomite (e.g., Valley & Essene 1980). Graphite from a calc-silicate sample (MP-3) has the highest  $\delta^{13}\text{C}$  of the Bissett



Creek samples (Table 3) and plots within the range of measured compositions from the Montpellier occurrence (Fig. 9). Therefore, the continuum of graphite  $\delta^{13}\text{C}$  compositions may represent a measure of the contribution of isotope exchange between organic carbon and carbonic fluids released during the breakdown of carbonate minerals during prograde metamorphism.

An alternative model to explain the continuum of  $\delta^{13}\text{C}$  for graphite at Bissett Creek is Rayleigh fractionation of metamorphic fluids derived from an initially homogeneous  $\delta^{13}\text{C}$  reservoir (e.g. Ray and Ramesh, 2000; Ray, 2009). Figure 10 presents the results of a multi-component Rayleigh fractionation model (Ray, 2009); this model considers graphite that precipitated from a mixed  $\text{CO}_2\text{--CH}_4$  metamorphic fluid at  $700^\circ\text{C}$  derived from a reservoir with  $\delta^{13}\text{C}$  of  $-26 \pm 2\text{‰}$ . The initial molar ratio of  $\text{CH}_4$  and  $\text{CO}_2$  ( $r_{\text{CH}_4\text{--CO}_2}$ ) in the source fluid was set at 0.99 to extend the evolution to a nearly complete exhaustion of the source (e.g. Ray, 2009).

Modeled graphite  $\delta^{13}\text{C}$  ranges from  $-32\text{‰}$  initially up to  $-17\text{‰}$  when 1% of the fluid remains (Fig. 10). Therefore, Rayleigh fractionation of an initially homogenous carbon reservoir can also explain the spread of  $\delta^{13}\text{C}$  at Bissett Creek. Considering the paucity of carbonate minerals and the relatively minor amount of calc-silicates at Bissett Creek, the Rayleigh fractionation model is our preferred interpretation for the continuum of  $\delta^{13}\text{C}$  of graphite from this locality.

The abundance of carbonate units at the Montpellier occurrence may have resulted in higher graphite  $\delta^{13}\text{C}$  than graphite from the carbonate-deficient Bissett Creek Deposit. Similar to Bissett Creek, however, the spread in  $\delta^{13}\text{C}$  of graphite may also represent Rayleigh fractionation of an initially homogeneous source. In either interpretation, the carbon responsible for graphite mineralization is mostly biotic in origin at both Montpellier and Bissett Creek.

Most studied graphite deposits in the southwestern Grenville Province are spatially associated with carbonate units (*e.g.*, Mackinnon and LeBaron 1990, 1992). The results of this study suggest that the source of carbon for graphite precipitation is principally biogenic even in the carbonate-rich Montpellier occurrence. Therefore, the contribution of carbon from the decarbonitization of carbonate minerals may be relatively minor. It remains to be tested if this holds true for other carbonate-hosted graphite deposits in the Grenville Province.

## CONCLUSIONS

The Bissett Creek deposit and the Montpellier showing in the southwestern Grenville Province contain disseminated graphite mineralization and graphite morphologies that are consistent with a metamorphic origin. Carbon isotope compositions of graphite from both deposits support a biogenic source for the carbon and the spread in graphite  $\delta^{13}\text{C}$  can be generated through a Rayleigh fractionation process. A minor contribution of carbon from the devolatilization of carbonate minerals is also possible at Montpellier. In general, the results of this study suggest that graphite deposits in the southwestern Grenville Province reflect graphite precipitation from metamorphic fluids derived from the breakdown of biogenic material.

## ACKNOWLEDGEMENTS

Mr. Greg Bowes, President of the Northern Graphite Corporation, Ottawa, has kindly authorized the authors to use all their available and confidential data. We thank W.M. Schwerdtner for his critical reading of an earlier version of this manuscript and J.S. Ray and an anonymous reviewer for thorough and constructive reviews. We thank Kim Law for assistance with the stable carbon isotope analyses, and acknowledge the Natural Sciences and Engineering Research Council of

Canada, the Canada Foundation for Innovation, the Ontario Research Fund and the Canada Research Chairs program for funding. This is Laboratory for Stable Isotope Science Contribution #353.

## REFERENCES

- BARKER, F. & FRIEDMAN, I. (1969) Carbon isotopes in pelites of the Precambrian Uncompahgre Formation, Needle Mountains, Colorado. *Geological Society of America Bulletin* **80**, 1403-1408.
- BARRENECHEA, J. F., LUQUE, F. J., MILLWARD, D., ORTEGA, L., BEYSSAC, O. & RODAS, M. (2009) Graphite morphologies from the Borrowdale deposit (NW England, UK): Raman and SIMS data. *Contributions to Mineralogy and Petrology* **158**, 37-51.
- BERNARD, S. & PAPINEAU, D. (2014) Graphitic carbons and biosignatures. *Elements* **10**, 435-440.
- BOUTTON, T.W. (1991) Stable carbon isotope ratios of natural materials. 1. Sample preparation and mass spectrometric analysis. In: Carbon Isotope Techniques. D.C. Coleman and B. Fry (eds.), 155-171, Academic Press, New York.
- BEYSSAC, O. & RUMBLE, D. (2014) Graphitic Carbon: A Ubiquitous, Diverse, and Useful Geomaterial. *Elements* **10**, 415-420.
- CARR, S. D., EASTON, R. M., JAMIESON, R. A. & CULSHAW, N. G. (2000) Geologic transect across the Grenville orogen of Ontario and New York. *Canadian Journal of Earth Sciences* **37**, 193-216.
- COPLEN, T. B., BRAND, W. A., GEHRE, M., GRÖNING, M., MEIJER, H. A. J., TOMAN, B. & VERKOUTEREN, R. M. (2006a) New guidelines for  $\delta^{13}\text{C}$  measurements. *Analytical Chemistry* **78**, 2439-2441.
- COPLEN, T. B., BRAND, W. A., GEHRE, M., GRÖNING, M., MEIJER, H. A. J., TOMAN, B. & VERKOUTEREN, R. M. (2006b) After two decades a second anchor for the VPDB  $\delta^{13}\text{C}$  scale. *Rapid Communications in Mass Spectrometry* **20**, 3165-3166.
- CRAWFORD, W. A. & VALLEY, J. W. (1990) Origin of graphite in the Pickering gneiss and the Franklin marble, Honey Brook Upland, Pennsylvania Piedmont. *Geological Society of America Bulletin* **102**, 807-811.
- DEINES, P. (2002) The carbon isotope geochemistry of mantle xenoliths. *Earth-Science Reviews* **58**, 247-278.
- DEINES, P., HARRIS, J. W., ROBINSON, D. N., GURNEY, J. J. & SHEE, S. R. (1991) Carbon and oxygen isotope variations in diamond and graphite eclogites from Orapa, Botswana, and the nitrogen content of their diamonds. *Geochimica et Cosmochimica Acta* **55**, 515-524.
- DUNN, S. R. & VALLEY, J. W. (1992) Calcite-graphite isotope thermometry: a test for polymetamorphism in marble, Tudor gabbro aureole, Ontario, Canada. *Journal of Metamorphic Geology* **10**, 487-501.

437 GALY, V., BEYSSAC, O., FRANCE-LANORD, C. & EGLINGTON, T. (2008) Recycling of graphite  
438 during Himalayan erosion: a geological stabilization of carbon in the crust. *Science* **322**,  
439 943-945.

440 GARLAND, M. I. (1987) *Graphite in the Central Gneiss Belt of the Grenville Province of Ontario*;  
441 *Ontario Geological Survey*, Ministry of the Northern Development and Mines Ontario  
442 Open File Report 5649, 275 pp.

443 GIGNAC, L., MARCHAND, R., MENARD, R., PHILLIPS, A., AIKEN, S. R., BOUAJILA, A., MENARD, N.,  
444 HOUDS, D., THIBERT, F., ROUSSEAU, G., CHAMPAGNE, A. (2012) *Feasibility study: Bissett*  
445 *Creek Graphite Project, Ontario, Canada*. Technical report by G Mining Service Inc. for  
446 Northern Graphite Corporation, 299 pp.

447 HAHN-WEINHEIMER, P. & HIRNER, A. (1981) Isotopic evidence for the origin of graphite.  
448 *Geochemical Journal* **15**, 9-15.

449 HEWITT, D.F. (1965) *Graphite in Ontario*. Ontario department of mines, Industrial Mineral  
450 Report no 20, 66 pp.

451 HORITA, J. (2001) Carbon isotope exchange in the system CO<sub>2</sub>-CH<sub>4</sub> at elevated temperatures.  
452 *Geochimica et Cosmochimica Acta* **65**, 1907-1919.

453 KEHELPANNALA, K. V. W. & FRANCIS, M. D. P. L. (2001) Vein graphite deposits of the Kegalle  
454 District, Sri Lanka: further evidence for post-metamorphic, fluid-deposited graphite.  
455 *Gondwana Research* **4**, 655-656.

456 KEITH, M. L. & WEBER, J. N. (1964) Carbon and oxygen isotopic composition of selected  
457 limestones and fossils. *Geochimica et Cosmochimica Acta* **28**, 1787-1816.

458 LANDIS, C. A. (1971) Graphitization of dispersed carbonaceous material in metamorphic rocks.  
459 *Contributions to Mineralogy and Petrology* **30**, 34-45.

460 LEDUC, M. (2013). *Preliminary Economic Assessment: NI 43-101FI TECHNICAL REPORT, for*  
461 *the Northern Graphite Corporation, Bissett Creek Project*. Prepared by AGP Mining  
462 Consultants Inc. 240 pp.

463 LUQUE, F. J., CRESPO-FEO, E., BARRENECHEA, J. F. & ORTEGA, L. (2012) Carbon isotopes of  
464 graphite: Implications on fluid history. *Geoscience Frontiers* **3**, 197-207.

465 LUQUE, F. J., HUIZENGA, J.-M., CRESPO-FEO, E., WADA, H., ORTEGA, L. & BARRENECHEA, J. F.  
466 (2014) Vein graphite deposits: geological settings, origin, and economic significance.  
467 *Mineralium Deposita* **49**, 261-277.

468 MACKINNON, A. & LEBARON, P.S. (1990) *Major Graphite Occurrences of the Frontenac Axis,*  
469 *Southeastern Ontario*. Ontario Geological Survey, Open File Report **5729**, 77pp.

470 MACKINNON, A. & LEBARON, P.S. (1992) *Graphite occurrences of the Frontenac axis, Eastern*  
471 *Ontario*. Ontario Geological Survey, Mineral Deposit circular **33**.

472 MITCHELL, C.J. (1993) *Industrial Minerals Laboratory Manual: Flake Graphite*. British  
473 Geological Survey Technical Report WG/92/30. 31 pages.

474 OKUYAMA-KUSUNOSE, Y. & ITAYA, T. (1987) Metamorphism of carbonaceous material in the  
475 Tono contact aureole, Kitakami Mountains, Japan. *Journal of Metamorphic Geology* **5**,  
476 121-139.

477 PAPINEAU, D., DE GREGORIO, B. T., CODY, G. D., FRIES, M. D., MOJZSIS, S. J., STEELE, A.,  
 478 STROUD, R. M. & FOGEL, M. L. (2010a) Ancient graphite in the Eoarchean quartz–  
 479 pyroxene rocks from Akilia in southern West Greenland I: Petrographic and  
 480 spectroscopic characterization. *Geochimica et Cosmochimica Acta* **74**, 5862-5883.

481 PAPINEAU, D., DE GREGORIO, B. T., STROUD, R. M., STEELE, A., PECOITS, E., KONHAUSER, K.,  
 482 WANG, J. & FOGEL, M. L. (2010b) Ancient graphite in the Eoarchean quartz-pyroxene  
 483 rocks from Akilia in southern West Greenland II: Isotopic and chemical compositions  
 484 and comparison with Paleoproterozoic banded iron formations. *Geochimica et*  
 485 *Cosmochimica Acta* **74**, 5884-5905.

486 PASTERIS, J. D. (1999) Causes of the uniformly high crystallinity of graphite in large epigenetic  
 487 deposits. *Journal of Metamorphic Geology* **17**, 779-787.

488 PEARSON, D. G., BOYD, F. R., HAGGERTY, S. E., PASTERIS, J. D., FIELD, S. W., NIXON, P. H. &  
 489 POKHILENKO, N. P. (1994) The characterisation and origin of graphite in cratonic  
 490 lithospheric mantle: a petrological carbon isotope and Raman spectroscopic study.  
 491 *Contributions to Mineralogy and Petrology* **115**, 449-466.

492 QI, H., COPLEN, T. B., GEILMANN, H., BRAND, W. A. & BÖHLKE, J. K. (2003) Two new organic  
 493 reference materials for  $\delta^{13}\text{C}$  and  $\delta^{15}\text{N}$  measurements and a new value for the  $\delta^{13}\text{C}$  of NBS  
 494 22 oil. *Rapid Communications in Mass Spectrometry* **17**, 2483-2487.

495 RAY, J. S. & RAMESH, R. (2000) Rayleigh fractionation of stable isotopes from a multicomponent  
 496 source. *Geochimica et Cosmochimica Acta* **64**, 299-306.

497 RAY, J. S. (2009) Carbon isotopic variations in fluid-deposited graphite: evidence for  
 498 multicomponent Rayleigh isotopic fractionation. *International Geology Review* **51**, 45-  
 499 57.

500 RIVERS, T., CULSHAW, N., HYNES, A., INDARES, A., JAMIESON, R. & MARTIGNOLE, J. (2012) The  
 501 Grenville Orogen—A post-Lithoprobe perspective *In* Tectonic styles in Canada: The  
 502 LITHOPROBE perspective. (J. A. PERCIVAL, F. A. COOK & R. M. CLOWES, EDS).  
 503 Geological Association of Canada Special Paper, 97–238.

504 RIVERS, T. & SCHWERDTNER, W. (2015) Post-peak Evolution of the Muskoka Domain, Western  
 505 Grenville Province: Ductile Detachment Zone in a Crustal-scale Metamorphic Core  
 506 Complex. *Geoscience Canada* **42**, 403–436.

507 RUMBLE, D. (2014) Hydrothermal Graphitic Carbon. *Elements* **10**, 427-433.

508 RUMBLE, D. & HOERING, T. C. (1986a) Carbon isotope geochemistry of graphite vein deposits  
 509 from New Hampshire, U.S.A. *Geochimica et Cosmochimica Acta* **50**, 1239-1247.

510 RUMBLE, D., DUKE, E. F. & HOERING, T. L. (1986b) Hydrothermal graphite in New Hampshire:  
 511 Evidence of carbon mobility during regional metamorphism. *Geology* **14**, 452-455.

512 SANGSTER, A. L., GAUTHIER, M. & GOWER, C. F. (1992) Metallogeny of structural zones,  
 513 Grenville Province, northeastern North America. *Precambrian Research* **58**, 401-426.

514 SANTOSH, M. & OMORI, S. (2008) CO<sub>2</sub> flushing: A plate tectonic perspective. *Gondwana*  
 515 *Research* **13**, 86-102.

516 SCHEELE, N. & HOEFS, J. (1992) Carbon isotope fractionation between calcite, graphite and CO<sub>2</sub>:  
517 an experimental study. *Contributions to Mineralogy and Petrology* **112**, 35-45.

518 SCHIDLowski, M. (1988) A 3,800-million-year isotopic record of life from carbon in sedimentary  
519 rocks. *Nature* **333**, 313-318.

520 SCHIDLowski, M. (2001) Carbon isotopes as biogeochemical recorders of life over 3.8 Ga of  
521 Earth history: evolution of a concept. *Precambrian Research* **106**, 117-134.

522 SCHULZE, D. J., VALLEY, J. W., VILJOEN, K. S., STIEFENHOFER, J. & SPICUZZA, M. (1997) Carbon  
523 isotope composition of graphite in mantle eclogites. *The Journal of Geology* **105**, 379-  
524 386.

525 SIMANDL, G.J. (1989) Inventaire de gites de graphite dans la région de Lachute-Hull-Mont-  
526 Laurier. Ministère de l'Énergie et des Ressources naturelles du Québec, MB 89-05, 21  
527 pp.

528 SOMAN, K., LOBZOVA, R. V. & SIVADAS, K. M. (1986) Geology, genetic types, and origin of  
529 graphite in South Kerala, India. *Economic Geology* **81**, 997-1002.

530 SPENCE, H.S. (1920) *Graphite*. Department of Mines, Canada, Publication no 511, 250 pp.

531 TANER, M.F. (1989) *Évaluation du potentiel en graphite de la propriété Ripon, dans le rang V et*  
532 *des lots 54 et 55 du canton Ripon, Comté de Papineau, Québec*. Ministère de l'Énergie et  
533 des Ressources naturelles du Québec, rapport GM 58585, 20 pp.

534 TANER, M.F. (2010) *Results of the 2010 Drilling Campaign for the Bissett Creek Graphite*  
535 *Property, Maria Township, Ontario (NTS 31 L/01)*. Northern Graphite Corporation, 93  
536 pp.

537 TANER, M.F. (2013) *Results of the 2012 Drilling Campaign for the Bissett Creek Graphite*  
538 *Property, Maria Township, Ontario (NTS 31 L/01)*. Northern Graphite Corporation, 112  
539 pp.

540 VALLEY, J. W. & ESSENE, E. J. (1980) Calc-silicate reactions in Adirondack marbles: The role of  
541 fluids and solid solutions: Summary. *Geological Society of America Bulletin* **91**, 114-117.

542 VILJOEN, K. S. (1995) Graphite- and diamond-bearing eclogite xenoliths from the Bellsbank  
543 kimberlites, Northern Cape, South Africa. *Contributions to Mineralogy and Petrology*  
544 **121**, 414-423.

545 WADA, H., TOMITA, T., MATSUURA, K., TUCHI, K., ITO, M. & MORIKIYO, T. (1994)  
546 Graphitization of carbonaceous matter during metamorphism with references to  
547 carbonate and pelitic rocks of contact and regional metamorphisms, Japan. *Contributions*  
548 *to Mineralogy and Petrology* **118**, 217-228.

549 WEIS, P. L., FRIEDMAN, I. & GLEASON, J. P. (1981) The origin of epigenetic graphite: evidence  
550 from isotopes. *Geochimica et Cosmochimica Acta* **45**, 2325-2332.

551 WYNNE-EDWARDS, H.R. (1972). The Grenville Province. In Variations in tectonic styles in  
552 Canad (R.A. PRICE & R.J.W. DOUGLAS, ED). Geological Association of Canada, 25<sup>th</sup>  
553 anniversary volume, Special Paper **11**: 263-334.

554

## FIGURE CAPTIONS

FIG. 1. Simplified map of the Grenville Province with the location of the Bissett Creek graphite deposit and the Montpellier graphite showing (modified from Rivers *et al.*, 2012). ABT: Allochthon Boundary Thrust, CABTZ: Composite Arc Boundary Thrust Zone, CAB: Composite Arc Belt, CGB: Central Gneiss Belt, FAB: Frontenac–Adirondack Belt, PSD: Parry Sound Domain.

FIG. 2. Field relationships of the Bissett Creek deposit. (a) Folded leucosome in the barren (no graphite) gneiss unit. (b) Gossan at the surface of a graphitic gneiss. (c) Pegmatite cutting foliation in the host graphitic gneiss. (d) Sub-vertical lamprophyre dyke cutting foliation in the host graphitic gneiss.

FIG. 3. Gneisses at the Bissett Creek deposit. (a) Biotite-rich quartzofeldspathic gneiss with graphite-rich melanosome. (b) Diopside-tremolite-biotite gneiss with graphite-rich melanosome. (c) Biotite-sillimanite-garnet gneiss with graphite- and biotite-rich melanosome. (d) Barren gneiss with pink leucosome.

FIG. 4. Microstructures of graphitic gneisses from the Bissett Creek deposit. (a) Quartzofeldspathic gneiss with disseminated graphite flakes (plane-polarized light). (b) Coarse-grained graphite in biotite-rich quartzofeldspathic gneiss (plane-polarized light). (c) Intergrown biotite and graphite in the biotite-rich quartzofeldspathic gneiss (plane-polarized light). (d) Disseminated graphite in a diopside–tremolite gneiss in plane polarized light (ppl; top left) and cross-polarized light (xpl; bottom right).

FIG. 5. Graphitic carbon contents of the two dominant graphitic units at the Bissett Creek deposit. Whiskers extend to the lowest and highest datum inside 1.5 times the interquartile range

FIG. 6. A simplified stratigraphic column of the geology of the Montpellier Graphite showing (modified from Taner 1989). 1. Impure quartzite, containing locally biotite-rich paragneiss (1a) and some monzonitic gneiss (1b). 2 Biotite–sillimanite–garnet-rich paragneiss with some graphite-rich zones. 3 Graphite rich zones (10 to 20 wt.% graphitic carbon). 4. Calc-silicate unit; (4a) containing 3-5 wt.% graphitic carbon; (4b) diopside-rich marble; (4c) marble. 5. Biotite-rich paragneiss without graphite flakes. 6 Hornblende and biotite-rich gneiss. 7. Granitic gneiss. 8. (Ortho-) amphibolite. 9. Late diabase dyke.

FIG. 7. Rock types and field relationships of the Montpellier Graphite showing. (a) An exposure of the main graphite-rich calc-silicate unit (UTM 4902260m E, 5077102m N; NAD83, Zone 17). Graphite is disseminated throughout the outcrop. (b) Recumbently folded calc-silicate unit (c) Irregular contact between the quartzite and paragneiss units.

FIG. 8. Microstructures of graphitic gneisses from the Montpellier graphite showing. (a) Combination of plane-polarized (ppl; top left) and cross-polarized (xpl; bottom right) images showing the association of carbonate minerals with graphite flakes in the calc-silicate unit. (b) Thin section scan showing disseminated graphite flakes in the calc-silicate unit (plane-polarized light). (c) Garnet associated with biotite and graphite in the paragneiss unit (plane-polarized

light). (d) Thin section scan showing coarse-grained graphite flakes intergrown with biotite (plane-polarized light). (e) Coarse-grained graphite in the graphite-rich zone (plane-polarized light). (f) Thin section scan (plane-polarized light) showing oriented graphite flakes in a graphite-rich layer.

FIG. 9. Summary of  $\delta^{13}\text{C}$  of graphite from Bissett Creek and Montpellier along with the variation in  $\delta^{13}\text{C}$  of different sources of carbon. The compositions of organic carbon (at  $\sim 1$  Ga) and recent marine carbonate are from Schidlowski (2001). The compositions of mantle graphite are compiled from Deines et al. (1991), Pearson et al. (1994), Viljoen (1995) and Schulze (1997). On the box-and-whisker plots, the whiskers extend to the lowest and highest datum inside 1.5 times the interquartile range and outliers are outside of this range.

FIG. 10. Results of a multicomponent Rayleigh fractionation model (Ray, 2009) for a starting source composition of  $\delta^{13}\text{C} = -26 \pm 2\text{‰}$ , a temperature of  $700^\circ\text{C}$  and  $r_{\text{CH}_4\text{-CO}_2} = 0.99$ . The graphite-fluid and  $\text{CO}_2\text{-CH}_4$  fractionation factors at this temperature are from Scheele and Hoefs (1992) and Horita (2001).



617 **TABLE 1.** Graphitic carbon contents of select samples from Bissett Creek.

618

Sample ID:	Rock Type	Graphitic C (wt. %)
BC03	Bt-Rich QF gneiss	1.29
BC11	Bt-Rich QF gneiss	3.63
BC12	Bt-Rich QF gneiss	3.15
BC13	Bt-Rich QF gneiss	3.16
BC14	Bt-Rich QF gneiss	2.92
BC15	Bt-Rich QF gneiss	3.88
BC16	Bt-Rich QF gneiss	2.76
BC17	Bt-Rich QF gneiss	0.86
BC18	Di-Trem gneiss	1.05
BC19	Pegmatite	1.38
BC20	Di-Trem gneiss	2.02
BC21	Di-Trem gneiss	1.33
BC22	Bt-Rich QF gneiss	1.36
BC23	Di-Trem gneiss	1.06
BC24	Di-Trem gneiss	1.98
BC25	Bt-Rich QF gneiss	2.01
BC26	Di-Trem gneiss	0.92
BC27	Bt-Rich QF gneiss	2.10
BC28	Di-Trem gneiss	2.01
BC29	Di-Trem gneiss	3.07

619

620

621

622

**TABLE 2.** Graphitic carbon content of samples from Montpellier.

Sample	Graphitic C (wt. %)
MPG-01	0.82
MPG-02	1.94
MPG-03	14.4
MPG-04	2.69
805	9.75
806	9.86
807	10.66
808	14.8
809	16.36
810	20.42
811	19.51

**TABLE 3.** Carbon isotope results for graphite from Bissett Creek and Montpellier.

Sample	Rock Type	$\delta^{13}\text{C}$ (‰, VPDB)
<i>Bissett Creek</i>		
BC-0	Bt-Rich QF gneiss	$-24.8 \pm 0.2$ (n=8)*
BC-M	Bulk sample from mill	$-21.2 \pm 0.2$ (n=2)
BC-10	Bt-Rich QF gneiss	$-29.1 \pm 0.1$ (n=3)
BC-11	Bt-Rich QF gneiss	$-18.8 \pm 0.7$ (n=3)
BC-12	Bt-Rich QF gneiss	$-26.7$ (n = 1)
BC-13B	Bt-Rich QF gneiss	$-17.4 \pm 0.2$ (n=3)
BC-14	Bt-Rich QF gneiss	$-22.5 \pm 0.6$ (n=4)
BC-15	Bt-Rich QF gneiss	$-20.2$ (n = 1)
<i>Montpellier</i>		
MP-2	Paragneiss	$-14.3 \pm 0.5$ (n=4)
MP-3	Calc-silicate gneiss	$-13.6$ (n = 1)
MP-4	Paragneiss	$-16.9 \pm 0.2$ (n=5)
MP-5	Paragneiss	$-17.7 \pm 0.2$ (n=5)

\*error reported as SD; n = number of analyses on graphite from each sample.

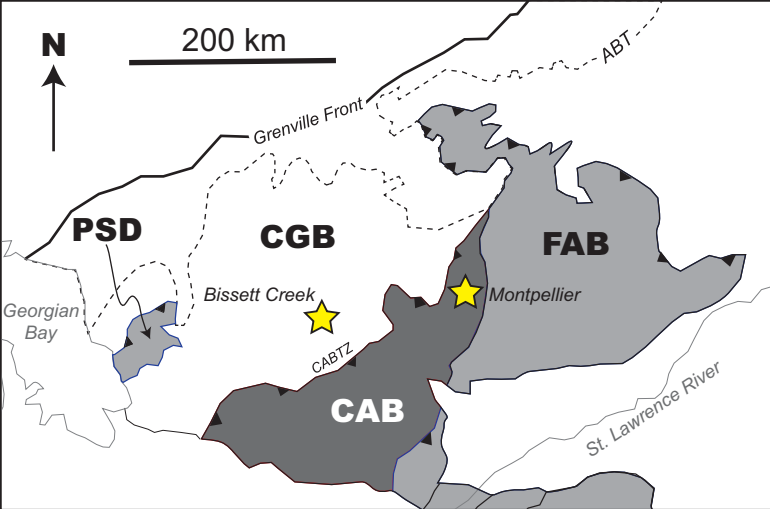


Figure 1



Figure 2



(a) Biotite-rich quartzofeldspathic gneiss



(b) Diopside-tremolite-biotite gneiss



(c) Biotite-sillimanite-garnet gneiss



(d) Barren gneiss

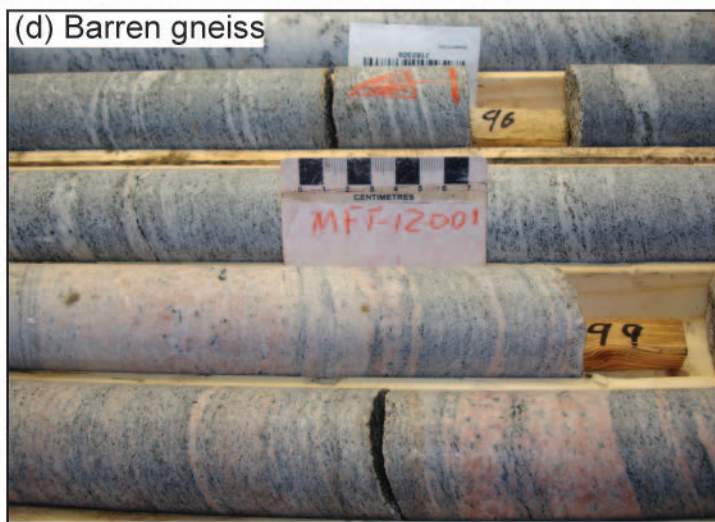


Figure 3



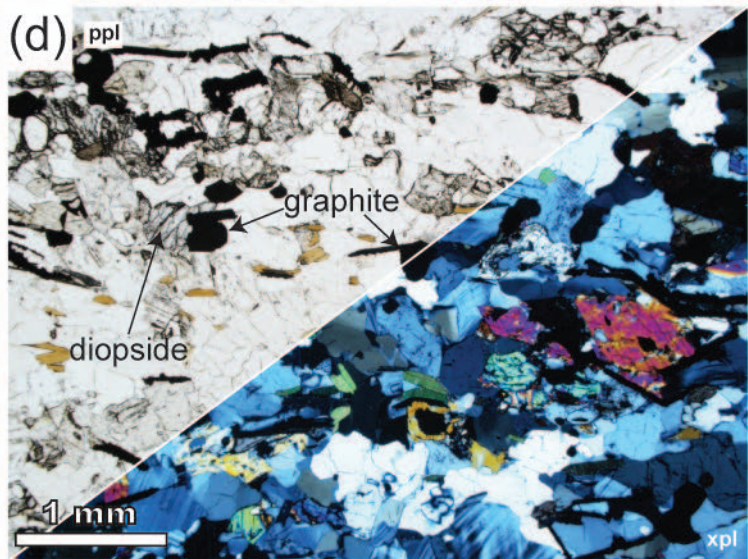
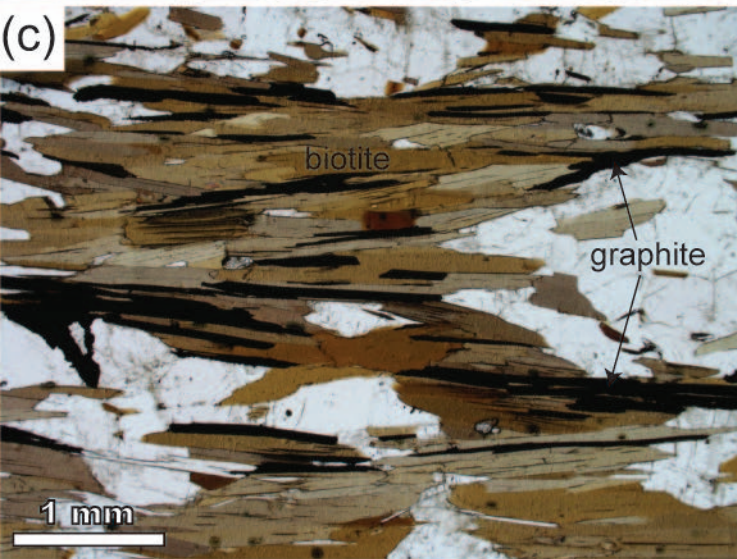
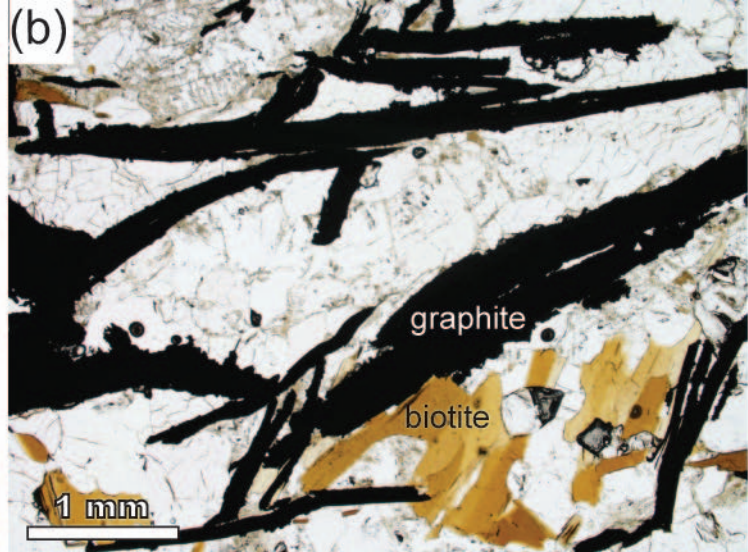
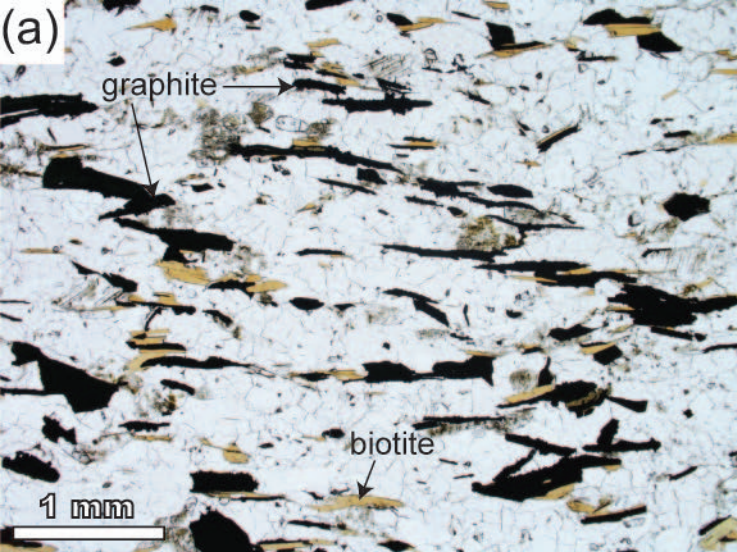


Figure 4

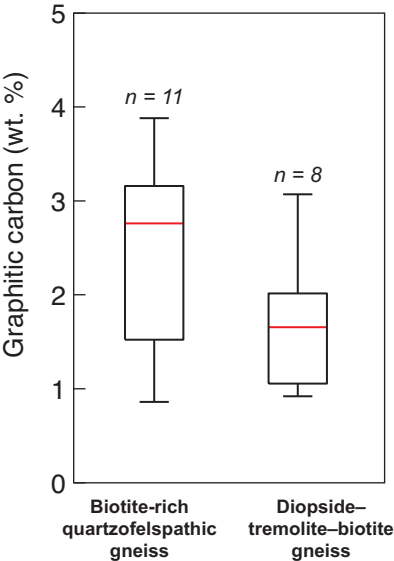


Figure 5

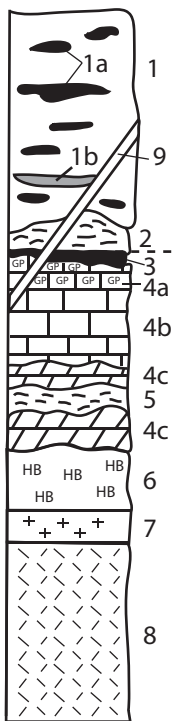


Figure 6



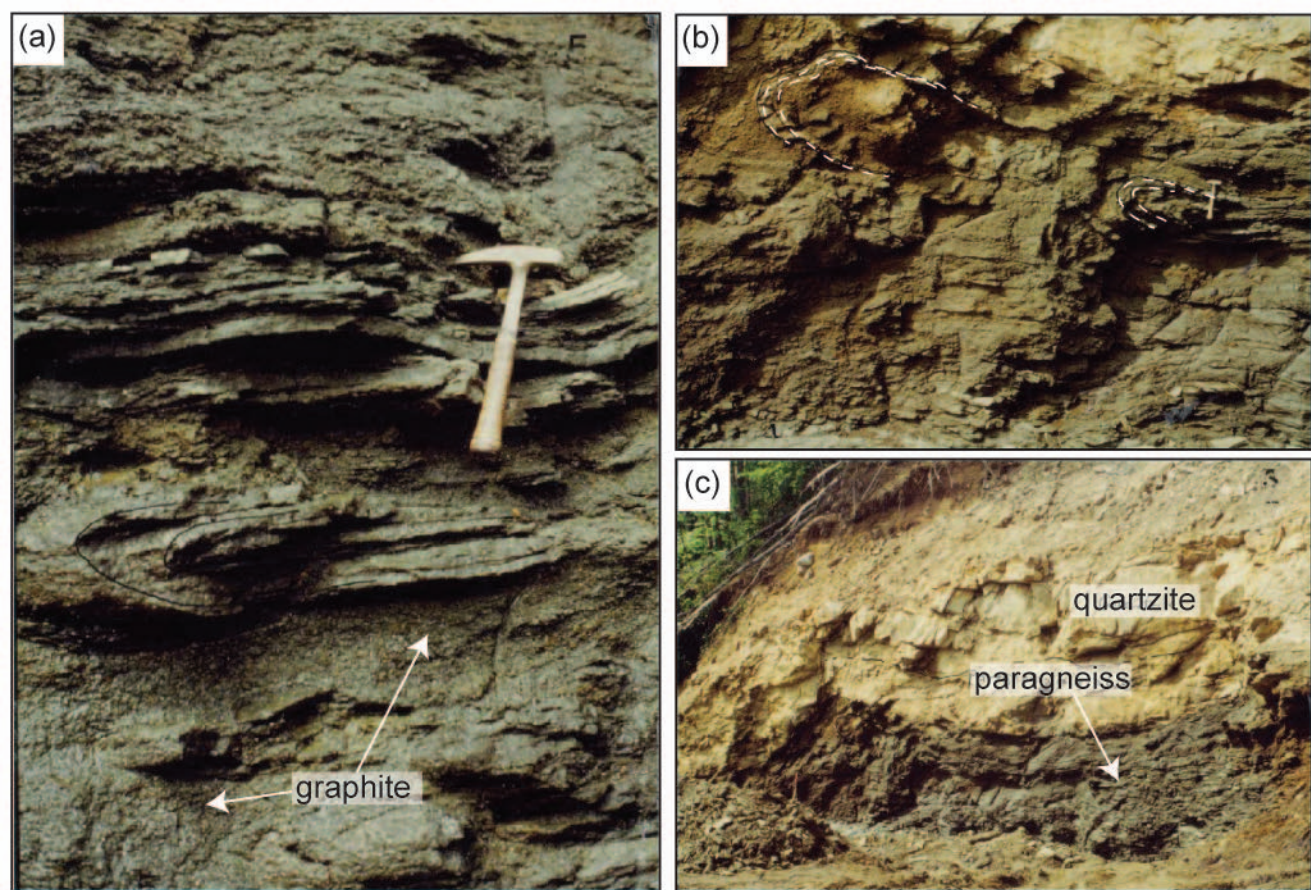


Figure 7



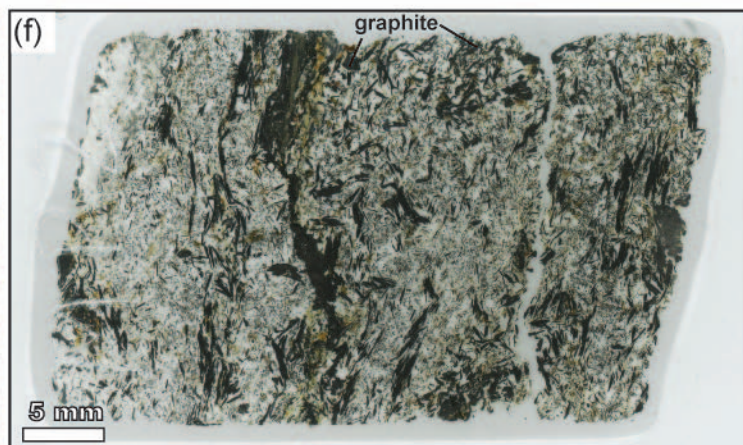
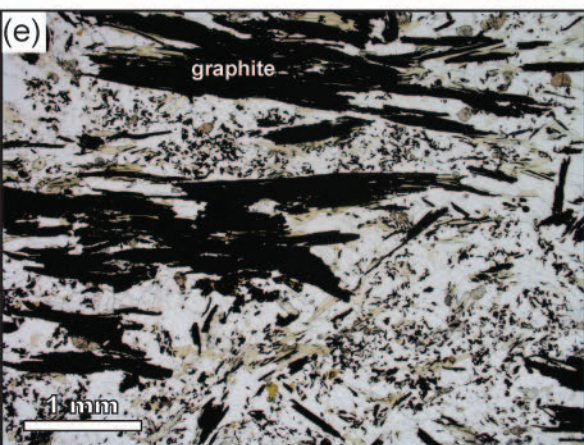
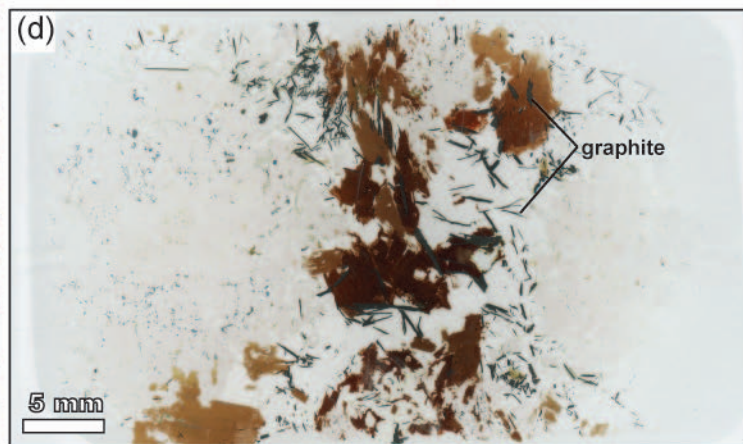
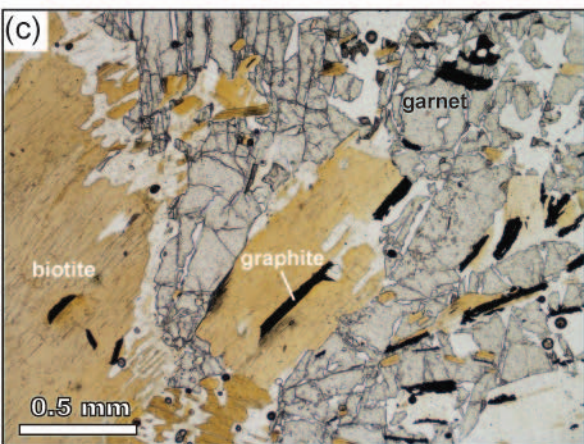
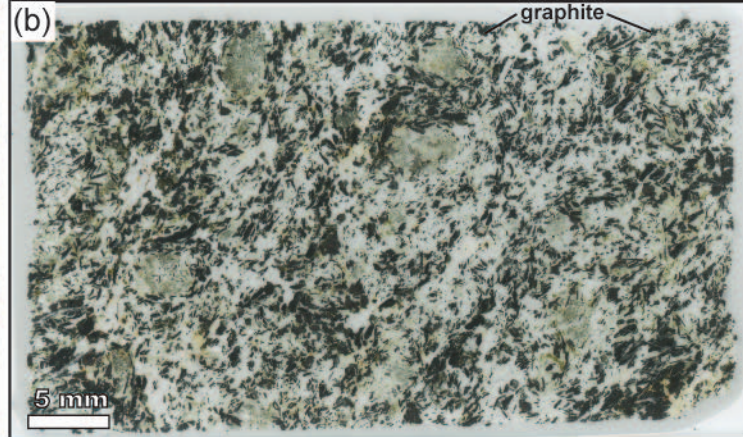
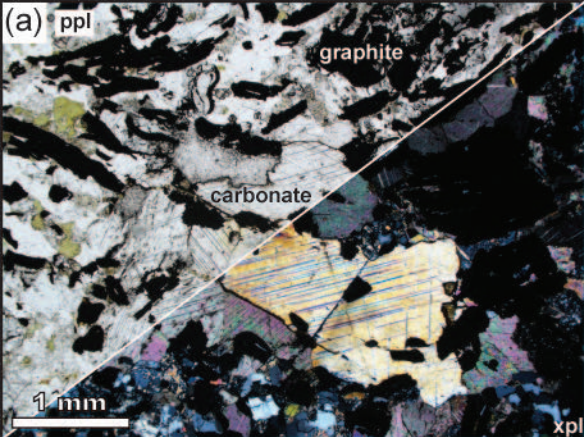


Figure 8

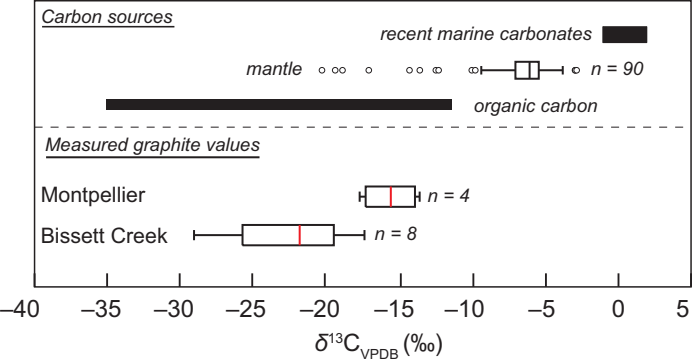
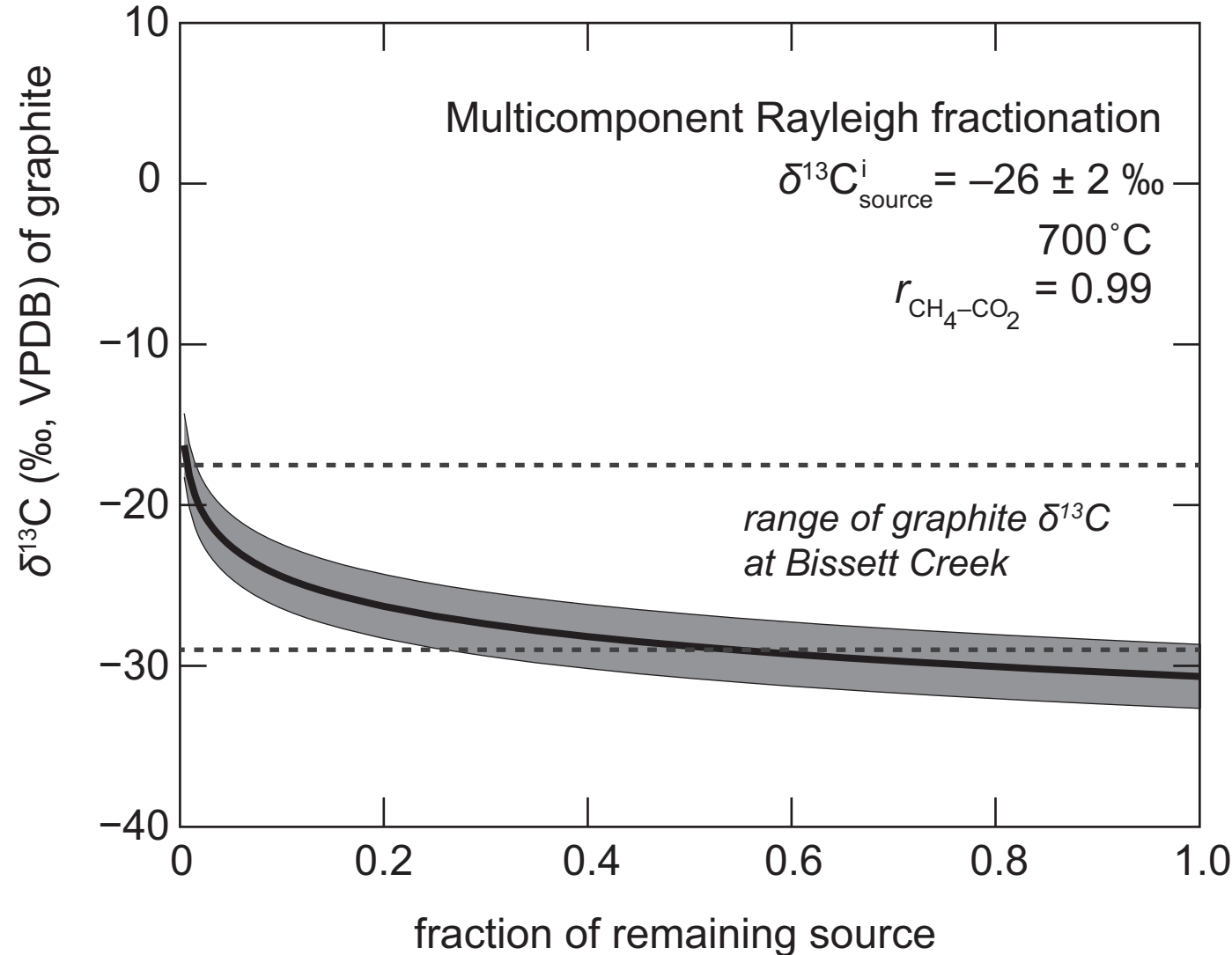


Figure 9



**Figure 10**